

## THREE-DIMENSIONAL BIOMECHANICAL AND VISUALISATION MODEL OF VERTIGO DISEASE IN THE SEMI-CIRCULAR CANAL

Žarko Milošević<sup>1,2,\*</sup>, Dalibor Nikolić<sup>1,2</sup>, Igor Saveljić<sup>1,2</sup>, Velibor Isailović<sup>1,2</sup>,  
Thanos Bibas<sup>3</sup>, Nenad Filipović<sup>1,2</sup>

<sup>1</sup> Faculty of Engineering, University of Kragujevac, Sestre Janjića 6,  
Kragujevac, Serbia

<sup>2</sup> BioIRC, Bioengineering Research and Development Center,  
Prvoslava Stojanovića 6, Kragujevac

<sup>3</sup> National & Kapodistrian University of Athens, 1st Department of  
Otolaryngology – Head & Neck Surgery, Athens, Greece

**Abstract:** Benign paroxysmal positional vertigo (BPPV) is the most common type of vertigo. The symptoms of BPPV typically appear after angular movements of the head. BPPV leads to dizziness, nausea and imbalance. In this study, we examined a model of the semi-circular canal (SCC) with fully 3D three dimensional anatomical data from specific patient. A full Navier-Stokes equations and continuity equations are used for fluid domain with Arbitrary-Lagrangian Eulerian (ALE) formulation for mesh motion of finite element. Fluid-structure interaction for fluid coupling with cupula deformation is used. Particle tracking algorithm is implemented for particle motion. Motion of the otoconia particles which is main cause for BPPV is simulated. Velocity distribution, shear stress and force from endolymph side are presented for patient specific three SCC. We compared our numerical models with experiments with head moving and nystagmus eye tracking. Numerical simulation can give more details and understanding of the pathology of the specific patient in standard clinical diagnostic and therapy procedure for BPPV.

**Keywords:** vertigo, semi-circular canals, otoconia particle, BPPV, biomechanical model, fluid-structure interaction.

### 1. INTRODUCTION

Balance problems often lead to falls [1], which is a pervasive but underinvestigated problem, partly due to the difficulties in determining the cause of the fall. The semi-circular canals are interconnected with the main sacs in the human ear: the utricle and the saccule which make up the otolith organs. Details on the vestibular system elements are presented in Figure 1.

BPPV is most common vestibular disorder. It originates from the presence of basophilic particles in the semicircular canals. These particles are displaced otoconia (calcium carbonate crystals) from the utricle and their motion is through semicircular canal system driven by gravity. BPPV has primary symptoms: nausea, dizziness, vertigo and ocular nystagmus. These symptoms are divided into two main categories: tonic and phasic. Tonic responses include maintained ocular nystagmus that is initiated immediately upon reorientation of the head relative

to gravity and it is called cupulolithiasis [2–4]. The second category are phasic symptoms which occur with a delayed onset and subside over time. It is called canalolithiasis, and it is typically attributed to the movement of free-floating particles within the lumen of the membranous labyrinth [5–12].

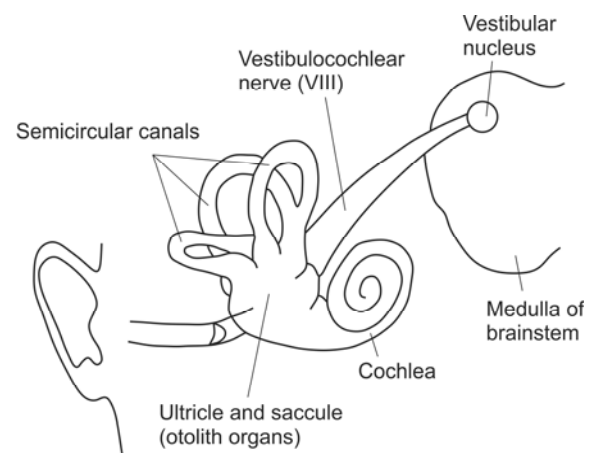


Figure 1. Vestibular system

\* Corresponding author: fica@kg.ac.rs

The most common diagnostic procedure for BPPV is the Dix-Hallpike head maneuver [13]. This maneuver tilts the head backward by about 120 degrees with the plane of rotation aligned with both the plane of the posterior SCC and the direction of gravity.

When cupula makes elastic feedback which results to post-rotatory cupula displacement, it triggers the misleading spinning sensation which is experienced during vertigo. Parnes & McClure [14] found free-floating particulate matter, mainly otolithic material, in the posterior canal of living BPPV patients. Canaliths consist of otoconia which detach from the utricular macula and enter the open-end of the SCC. The majority of the BPPV patients can be cured by so called repositioning head maneuvers [15–18]. These head maneuvers consist of several reorientations of the patient's head with the goal to move canaliths out of the narrow SCC and into the bigger utricle.

The weakness of the one canal approach is that it does not account for fluid coupling between

canals and it is unable to describe the role of the semicircular canal geometry in responses to complex 3-D head movements. In this paper we presented 3D model for real patient geometry by full fluid-structure interaction approach for particle, wall, cupula deformation and endolymph flow. We described numerical procedures for parametric and 3D SCC finite element solver with fluid-structure interaction. Some results for fully three SCC from real patients are given. Finally, we compared some numerical results with experimental measurement.

## 2. METHODS

BPPV is diagnosed by tracking the eye movements during and after a head maneuver (nystagmus). The nystagmus aims to compensate any angular motion in order to stabilize our vision. It is an indicator for the perceived angular velocity. Fluid mechanics and sedimenting particles tracking in a SCC are schematically presented in Figure 2.

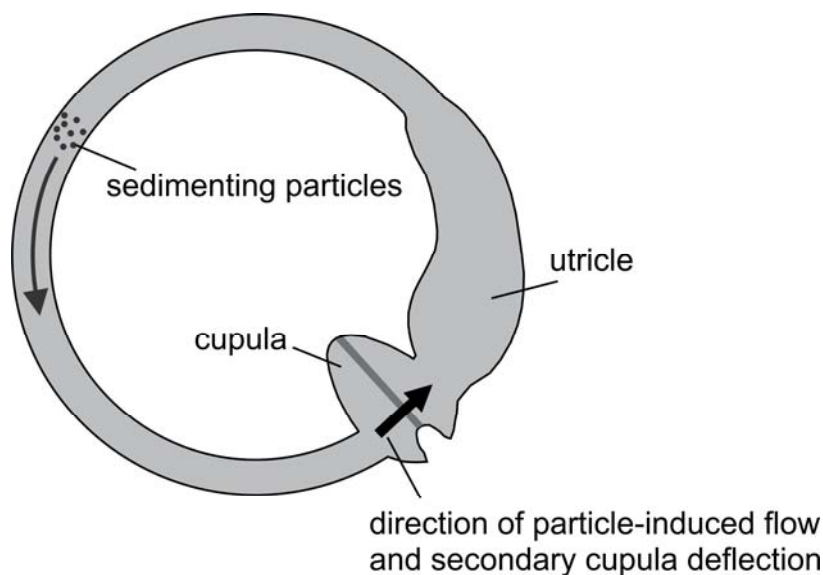


Figure 2. Fluid mechanics and sedimenting particles tracking in a semicircular canal

### 2.1. Fluid domain formulation

For fluid domain, the full 3D Navier-Stokes equation and continuity equation are used. To eliminate the pressure calculation in the velocity-pressure formulation, Penalty method is implemented [19]. The procedure is as follows. The continuity equation is approximated as

$$v_{i,i} + \frac{p}{\lambda} = 0 \quad (1)$$

where  $\lambda$  is a selected large number, the penalty

parameter. Substituting the pressure  $p$  from Eq. 1 into the Navier-Stokes equations we obtain

$$\rho \left( \frac{\partial v_i}{\partial t} + \partial v_{i,k} v_k \right) - \lambda v_{j,ij} - \mu v_{i,kk} - f_i^V = 0 \quad (2)$$

then the FE equation of balance becomes

$$\mathbf{M}\dot{\mathbf{V}} + (\mathbf{K}_{vv} + \mathbf{K}_{vv}^\lambda) \mathbf{V} = \mathbf{F}_v + \mathbf{F}_\lambda \quad (3)$$

where

$$[\mathbf{K}_{KJ}^\lambda]_{ik} = \lambda \int_V N_{K,i} N_{J,k} dV, \quad (\mathbf{F}_\lambda)_{Ki} = \lambda \int_S N_K v_{j,j} n_i dS \quad (4)$$

There are many conditions in science, engineering and bioengineering where fluid is acting on a solid producing surface loads and deformation of the solid material. The opposite also occurs, i.e. deformation of a solid affects the fluid flow. There are, in principle, two approaches for the Finite Element (FE) modeling of solid-fluid interaction problems: a) strong coupling method, and b) loose coupling method. In the first method, the solid and fluid domains are modeled as one mechanical system. In the second approach, the solid and fluid are modeled separately and the solutions are obtained with different FE solvers, but the parameters from one solution which affect the solution for the other medium are transferred successively. If the loose coupling method is employed, the systems of balance equations for the two domains are formed separately and there are no such computational difficulties. Hence, the loose coupling method is advantageous from the practical point of view and we further describe this method. As stated above, the loose coupling approach consists of the successive solutions for the solid and fluid domains [20].

We implemented fluid-structure interaction for cupula deformation and endolymph flow. Cupula was modeled as elastic 3D membrane with brick finite element and endolymph domain as 3D 8-node finite elements.

## 2.2. ALE (Arbitrary Lagrangian Eulerian) formulation

For mesh movement, ALE (Arbitrary Lagrangian Eulerian) formulation is implemented. In an incremental analysis, a linearization with respect to time must be performed using the known values at the start of a time step  $n$ . The approximation for a quantity  $F$  can be written as:

$${}^{n+1}F \Big|_{n\xi} = {}^nF \Big|_{n\xi} + F^* \Delta t \quad (5)$$

This relation is further applied to the left and right hand sides, (LHS) and (RHS), to obtain

$${}^n(LHS) + (LHS)^* \Delta t = {}^{n+1}(RHS) \quad (6)$$

In calculating the mesh-referential time derivatives we use the relations:

$$\left( \frac{\partial F}{\partial x_i} \right)^* = \frac{\partial F^*}{\partial x_i} - \left( \frac{\partial v_k^m}{\partial x_i} \right) \frac{\partial F}{\partial x_k} \quad (7)$$

and

$$(dV)^* = \frac{\partial v_k^m}{\partial x_k} dV \quad (8)$$

With these linearizations the governing

equations of fluid motion can be written as [30]

$${}^n \mathbf{M}_{(1)} \mathbf{V}^* + {}^n \mathbf{K}_{(1)vv} \Delta \mathbf{V} + {}^n \mathbf{K}_{vp} \Delta \mathbf{P} = {}^{n+1} \mathbf{F}_{(1)} - {}^n \mathbf{F}_{(1)} \quad (9)$$

and

$${}^n \mathbf{M}_{(2)} \mathbf{V}^* + {}^n \mathbf{K}_{(2)vv} \Delta \mathbf{V} = {}^{n+1} \mathbf{F}_{(2)} - {}^n \mathbf{F}_{(2)} \quad (10)$$

The integrals are evaluated over the known FE volumes and surfaces at start of time step. Further, some of the terms are calculated using the values at the last iteration. Of course, the mesh-referential time derivatives  $\mathbf{V}^*$  and  $\mathbf{P}^*$  are replaced by  $\mathbf{V}^* = \Delta \mathbf{V} / \Delta t$  and  $\mathbf{P}^* = \Delta \mathbf{P} / \Delta t$  to obtain the incremental algebraic equations.

The presented formulation of the FE modeling is necessary when the fluid boundaries change significantly over the time period used in the analysis. It is particularly convenient when the boundary of the fluid represents a deformable solid, for appropriate modeling the solid-fluid interactions. Finally, it is worth noting that the mesh motion is arbitrary and it can be specifically designed for each problem. As well, it is important to emphasize that the solution for the fluid flow does not depend on the FE mesh motion [20].

## 2.3. Particle tracking algorithm

Otoconia particle was modeled as single particle with corresponding volume which occupied one or more 3D 8-node finite elements. In this way we have also hydrodynamic influence from particle on fluid as fluid on particle which is fully coupled model.

The first step in the particle tracking algorithm is determining which finite element contains a specified point. The coordinates of a point can be divided into their integer and fractional parts:  $\vec{x} = (x, y, z) = [i, j, k] + (\alpha, \beta, \gamma)$ , where  $i, j, k$  are integers and  $\alpha, \beta, \gamma \in [0, 1]$ . In many texts  $[i, j, k]$  are referred to as indices and  $(\alpha, \beta, \gamma)$  as offsets. Point location is as simple as truncating the coordinates to their integer parts. The integer parts give the finite element where the point is located. Here, determining the offsets is also considered to be part of the point location operation, but sometimes we will strictly distinguish between point location and offset determination. The offsets are used to make a weighted interpolation.

The velocity at the current position of the particle is required to advance the particle. In order to obtain a value of the velocity field at points other than the grid nodes, it is necessary to determine an interpolated value using the velocities at the nodes of the finite element that contains the point.

### 3. RESULTS

Fluid velocity distribution for real patient specific geometry of three SCC for prescribed head motion is presented in Figure 3. A 3D reconstruction was done

with our software platform from original DICOM images. A user can prescribe a different head motion and see the response for all three SCC with numerical results as shear stress distribution, velocity, cupula deformation and drag force on the wall.

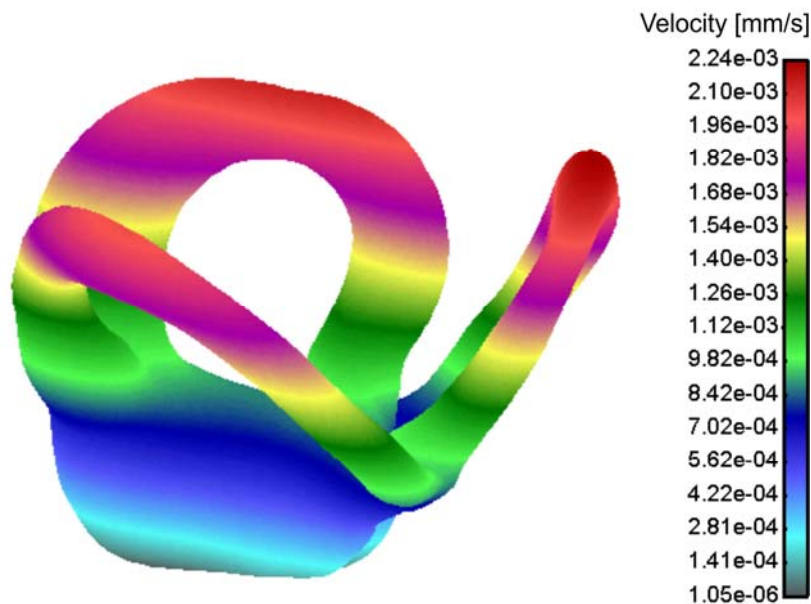


Figure 3. Fluid velocity distribution for real patient specific geometry of three SCC for prescribed head motion

The corresponding head motion with canalith repositioning procedures moves the endolymph in HC duct. The velocity in the two vertical SSC is also generated. The flow induces the HC cupula deformation due to fluid forces which act on the cupula wall. Shear stress distribution is shown in Figure 4.

It can be seen that more dominant maximum shear stress distribution is presented on the cupula walls. Simulation of the particles motions, velocity fluid distribution and cupula deformation is presented in Figure 5.

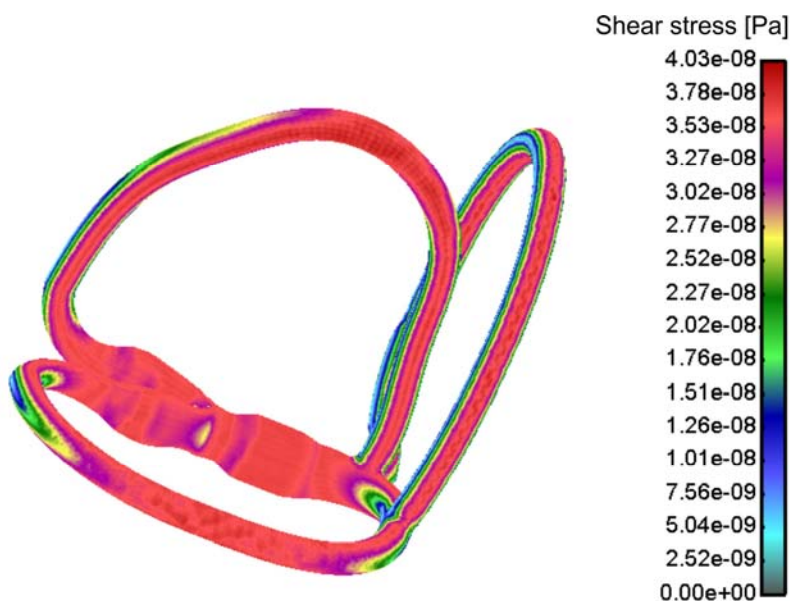


Figure 4. Shear stress distribution

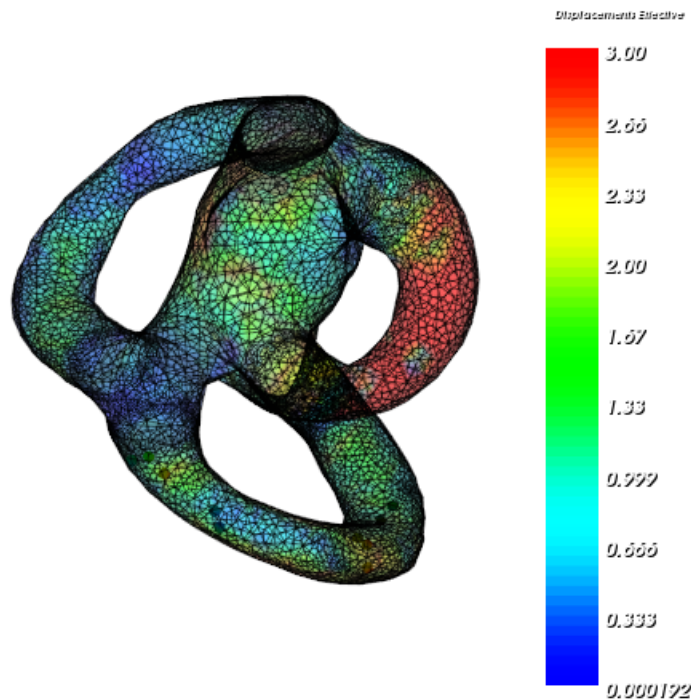


Figure 5. Simulation of the particles motions, velocity fluid distribution and cupula deformation

Comparison with numerical model of one SCC with cupula deformation and three sedimenting particles which are moved inside the fluid domain and eye tracking motion is done during the Dix-Hallpike test [13] for BPPV (Figure 6). A person is brought from sitting to a supine position, with the head turned 45 degrees to one side and extended about 20 degrees backward. Once supine, the eyes are typically observed for about 30 seconds. If no nystagmus ensues, the person is brought back to sitting. There is a delay of about

30 seconds again, and then the other side is tested.

Numerical model of fluid-structure interaction with endolymph fluid and cupula membrane solid domain was implemented. Also, particle tracking algorithm for otoconia particle motion as well as fluid-structure interaction with particle-fluid domain is used.

Numerical and experimental solution for cupula deformation for head manoeuvre is presented in the Figure 6.

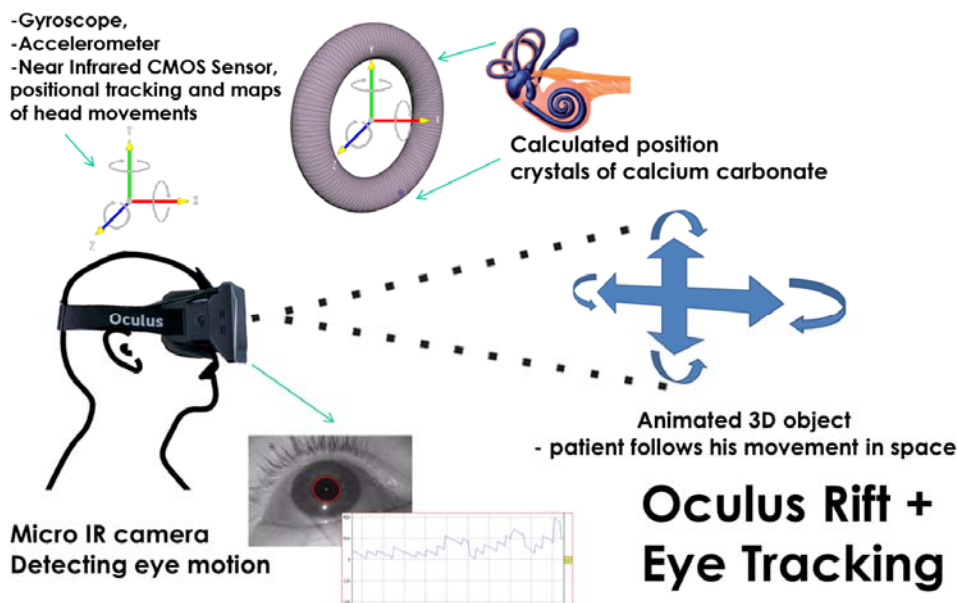


Figure 6. Numerical and experimental solution for head manoeuvre

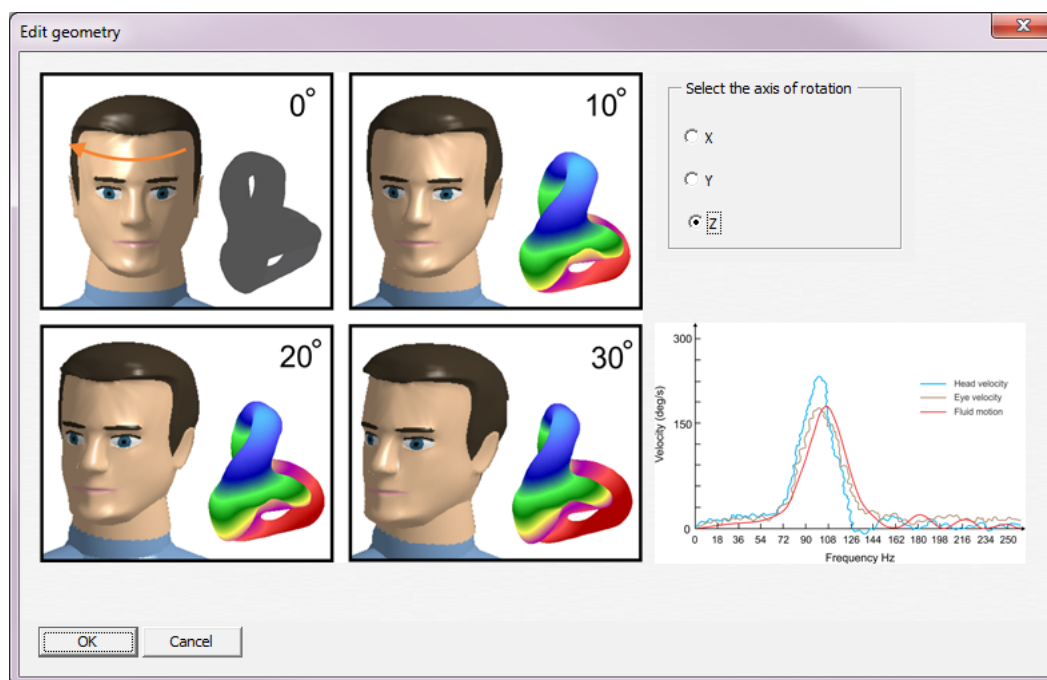


Figure 7. Numerical and experimental solution for head test movement, head velocity, eye velocity and fluid motion velocity

Some of the comparison for numerical and experimental solution for head test movement, head velocity, eye velocity and fluid motion velocity are presented in Figure 7.

#### 4. DISCUSSION AND CONCLUSION

In this paper, we presented a full three-dimensional mathematical model of the semi-circular canal. The main focus is on the BPPV, with sedimenting floating particle within the lumen of the membranous labyrinth. This approach gives more physiologically realistic description of the SCC, fluid motion, otoconia interaction with wall, fluid and cupula as well as cupula elastic deformation. Inside fluid domain, we can simulate vortices inside the utricle and ampula which is almost impossible in the current models from the literature. It is also easy to implement nonlinear behavior of cupula deformation when experimental data for material model description will be available. We presented different simulation results for patient specific three SCC. Finally, there are some comparisons of numerical results and measurements using video tracking head and eye movement system. It can open a new avenue for better diagnostic process for balance disorder disease.

#### 5. ACKNOWLEDGEMENTS

This research is supported by the grants: EC FP7 610454 EMBalance project, III41007 and

ON174028 Ministry of Education, Science and Technological Development of Serbia.

#### 6. REFERENCES

- [1] A. Berthoz, *The sense of movement*. Harvard University Press. (2002).
- [2] E. Mach, *Grundlinien der Lehre ion den Bewegungsempfindungen*. Leipzig: Wilhelm Engelmann. (1875).
- [3] J. D. Dickman, *Spatial orientation of semicircular canals and afferent sensitivity vectors in pigeons*, Exp. Brain Res., Vol. 111-1 (1996) 8-20.
- [4] H. F. Schuknecht, *Positional vertigo: clinical and experimental observations*, Trans Am Acad Ophthalmol Otol, Vol. 66 (1962) 319-331.
- [5] J. M. Epley, *The canalith repositioning procedure: for treatment of benign paroxysmal positional vertigo*, Otolaryngol Head Neck Surg., Vol. 107 (1992) 399-404.
- [6] S. F. Hall, R. R. Ruby, J. A. McClure, *The mechanics of benign paroxysmal vertigo*, J Otolaryngol, Vol. 8 (1979) 151-158.
- [7] L. S. Parnes, J. A. McClure, *Free-floating endolymph particles: a new operative finding during posterior semicircular canal occlusion*, Laryngoscope, Vol. (1992) 988-992.
- [8] G. De la Meilleure, I. Dehaene, M. Depondt, W. Damman, L. Crevits, G. Vanhooren, *Benign paroxysmal positional vertigo of the hori-*

zontal canal, *J Neurol Neurosurg Psychiatry*, Vol. 60 (1996) 68–71.

[9] J.M. Furman, S. P. Cass, B. C. Briggs, *Treatment of benign positional vertigo using heels-over-head rotation*, *Ann Otol Rhinol Laryngol*, Vol. 107 (1998) 1046–1053.

[10] T. Lempert, K. Tiel-Wilck, *A positional maneuver for treatment of horizontal-canal benign positional vertigo*, *Laryngoscope*, Vol. 106 (1996) 476–478.

[11] T. Lempert, *Horizontal benign positional vertigo*, *Neurology*, Vol. 44 (1994) 2213–2214.

[12] D. Nuti, G. Agus, M. T. Barbieri, D. Passali, *The management of horizontal-canal paroxysmal positional vertigo*, *Acta Otolaryngol*, Vol. 118 (1998) 455–460.

[13] M. R. Dix, C. S. Hallpike, *The pathology, symptomatology and diagnosis of certain common disorders of the vestibular system*, *Proc. R. Soc. Med.*, Vol. 45–6 (1952) 341–354.

[14] L. S. Parnes, J. A. McClure, *Free-floating endolymph particles: A new operative finding during posterior semicircular canal occlusion*, *Laryngoscope*, Vol. 102–9 (1992) 988–992.

[15] J. Epley, *The canalith repositioning procedure: for treatment of benign paroxysmal positional vertigo*, *Otolaryngol. Head Neck Surg.*, Vol. 107–3 (1992).

[16] A. Semont, G. Freyss, E. Vitte, *Curing the BPPV with a liberatory maneuver*, *Otorhinolaryngol.* (1988) 42.

[17] L. Parnes, R. Price-Jones, *Particle repositioning maneuver for benign paroxysmal positional vertigo*, *Ann. Otol. Rhinol. Laryngol.*, Vol. 102–5 (1993).

[18] T. A. Ghanem, R. D. Rabbitt, P. A. Tresco, *Three dimensional reconstruction of the membranous vestibular labyrinth in the toadfish*, *Opsanus tau. Hear Res.*, Vol. 124–1/2 (1998) 27–43.

[19] N. Filipović, S. Mijailović, A. Tsuda, M. Kojić, *An Implicit Algorithm within the Arbitrary Lagrangian-Eulerian Formulation for Solving Incompressible Fluid Flow with Large Boundary Motions*, *Comp. Meth. Appl. Mech. Engrg.*, Vol. 195 (2006) 6347–6361.

[20] M. Kojić, K. J. Bathe, *Inelastic Analysis of Solids and Structures*, Springer-Verlag, Berlin-Heidelberg 2005.



#### ТРОДИМЕНЗИОНАЛНИ БИОМЕХАНИЧКИ И ВИЗУЕЛНИ МОДЕЛ ГЛАВОБОЉЕ У ПОЛУЦИРКУЛАРНИМ КАНАЛИМА

**Сажетак:** Бенигна пароксимална позициона вртоглавица (БППВ) најчешћи је тип вртоглавице. Симптоми БППВ поремећаја обично се појављују после кружног кретања главе код пацијената. Овај поремећај води ка вртоглавици, мучнини и неравнотежи. У раду је компјутерски анализиран модел полуциркуларних канала са пуним тродимензионим анатомским подацима од одређеног пацијента. Пуне Навије-Стоксове једначине и једначина континуитета су коришћене за домен флуида са произвољном Лагранж-Ојлеровом формулацијом за кретање мреже коначних елемената. За деформацију купуле коришћена је солид-флуид интеракција. За кретање честица је примењен посебан алгоритам за праћење. Кретање честица отоконије главни је узрок БППВ поремећаја. Приказани су резултати распореда брзина флуида, смичућих напона и сила са стране ендолимфе. Поредили смо нумеричка решења са експерименталним подацима кретања главе и покрета очију. Нумеричке симулације могу дати више детаља и разумевања у патологији сваког пацијента понаособ у стандардној клиничкој процедури дијагностике и терапије за БППВ поремећај.

**Кључне речи:** вртоглавица, семи-циркуларни канали, честице отоконије, БППВ, солид-флуид интеракција.

